EVALUATION OF PRESSURE DISTRIBUTIONS ON AN AIRCRAFT BY TWO DIFFERENT PANEL METHODS AND COMPARISON WITH EXPERIMENTAL MEASUREMENTS

A. Baston, M. Lucchesini, L. Manfriani
Aerodynamic & Flight Mechanics Dept.,
Aermacchi S.p.A. - Varese

L. Polito, G. Lombardi
Aerospace Engineering Dept.,
University of Pisa

Abstract

Some years ago Morino proposed a new formulation of the problem of the potential flow around complex configurations, which seems to offer some advantages over the classical first-order panel methods.

This paper presents a comparison between the results obtained from a "first-order singularity" panel program in use at Aermacchi (NLR program) and a program based on Morino's theory developed by two of the authors at the "University of Pisa".

The comparison is based on a realistic, rather complex fighter aircraft configuration for which extensive wind tunnel data are available; a number of discretized geometry schemes with different degrees of refinement have been used, and an attempt has been made to compare realistically the computer usages in terms of time and memory occupation.

The results obtained refer to the pressure and load distributions on the fuselage at Mach= 0.7 and on the wing at Mach = 0.5.

1. Introduction

Panel methods are presently one of the most useful and practical tools for the aerodynamic design of aircrafts. A wide variety of programs has been developed, and most of them are routinely used in the industry with good success.

Morino[1] proposed a new formulation of the problem of the potential flow around complex configurations, which differs from the other methods mainly in that the potential function on the wetted surface is the main unknown; however a program based on this concept is generally similar to the other "panel methods" as to geometry description and discretization.

An advantage of Morino's formulation over the classical first-order methods appears to be the lower number of unknowns needed to achieve a satisfactory degree of accuracy.

The results presented in[2] actually show that a computer code based on this "potential method" may be a cost-effective alternative to more complex, higher order methods, at least as far as simple geometries are concerned.

The existing literature on this method is mostly concerned with the theoretical aspects or the treatment of simple cases, while nothing can be found on the relative merits of Morino's formulation when applied to practical complex configurations.

This paper is meant to fill this gap by presenting a comparison between the results obtained from a first-order panel method (NLR[3]) and a program (S-SUB2) based on Morino's theory[4].

The comparison is based on a realistic, rather complex fighter aircraft configuration for which extensive wind tunnel data are available (see fig. 4).

Four discretized geometry schemes with different degrees of refinement have been used to ascertain the sensitivity of the two methods to the number of panels and to compare computer usages in term of time and memory occupation.

2. Theoretical and numerical main features of the two panel methods

The NLR method[3] and Morino's method [1,4], in its subsonic steady state version, share the same theoretical basis, i.e. the classical linearized equation for the perturbation velocity potential φ:

$$(1-M_\infty^2)\,\varphi_{xx} + \varphi_{yy} + \varphi_{zz} = 0, \qquad (1)$$

with the boundary conditions:

$$\partial\varphi/\partial n = -\vec{U}_\infty \cdot \vec{n} \quad \text{on the body} \qquad (2\text{-a})$$

$$\varphi = 0 \quad \text{in the unperturbed flow} \qquad (2\text{-b})$$

The meaning of the symbols is the following: $\vec{U}_\infty$ and M_∞ are respectively the free stream velocity and the Mach number; x, y, z are the spatial Cartesian coordinates; $\vec{n}$ is the unit vector normal to the body surface. The x axis is assumed to be parallel to the free stream.

Equation(1) for $M_\infty < 1$ can be reduced to the well known Laplaces' equation :

$$\nabla^2\varphi = 0 \qquad (3)$$

where ∇ is the gradient operator ($\partial/\partial x$, $\partial/\partial y$, $\partial/\partial z$), thanks to Prandtl-Glauert formulae which transform the physical space into an incompressible analogous space, or P.G. space.

2.1. Theoretical considerations

Equation(1) is obtained by neglecting the non-linear and time-dependent terms contained in the full-potential equation :

$$\nabla^2\Phi - \frac{1}{a_\infty^2}\left(\frac{\partial}{\partial t} + U_\infty \frac{\partial}{\partial x}\right)^2\Phi = M_\infty^2\, G \qquad (4\text{-a})$$

with the non linear part:

$$G = 2\,\Phi_x\,\Phi_{xx} + (\Phi^2_x, \Phi^2_y, \Phi^2_z)\cdot(\Phi_{xx}, \Phi_{yy}, \Phi_{zz}) +$$

$$2\,(\Phi_y\,\Phi_{xy} + \Phi_z\,\Phi_{xz}) + 2(\Phi_x\,\Phi_y, \Phi_x\,\Phi_z, \Phi_y\,\Phi_z)\cdot$$

$$(\Phi_{xy}, \Phi_{xz}, \Phi_{yz}) + 2\,\nabla\Phi\cdot\nabla\Phi_t/U_\infty +$$

$$(\gamma - 1)\,(\Phi_t/U_\infty + \Phi_x + |\nabla\Phi|^2/2)\nabla^2\Phi \qquad (4\text{-b})$$

where $U_\infty = |\vec{U}_\infty|$, $\Phi = \varphi/U_\infty$, $a_\infty = U_\infty/M_\infty$, t = time, γ = ratio of specific heats, $\cdot$ denoting the scalar product. The boundary conditions for equations(4), corresponding to equations(2), are :

$$\partial S/\partial t + (\vec{U}_\infty + \nabla\varphi)\cdot\nabla S = 0 \text{ on the body} \qquad (5\text{-a})$$

$$\varphi = 0 \text{ in the unperturbed flow,} \qquad (5\text{-b})$$

where equation(5-a) states the condition the fluid should never cross the surface of the configuration described by the shape equation S (x, y, z, t) = 0.

Neglecting the non-linear terms, eq.(4-a) reduces to the acoustic equation or, neglecting the compressibility, to eq.(3) for (in general) time-dependent φ.

Equations(4) are of fundamental importance in Morino's theory as they allow the use of just one method for steady, unsteady, subsonic, transonic and supersonic flow. By applying Green's theorem the differential eq.(4-a) yields an integral expression which, for $M_\infty < 1$ and the motion of the surface assumed as infinitesimal, is :

$$4\pi E(P)\,\Phi(P,t) = \int_{S_B} -\psi'\frac{dS}{R} + \int_{S_B} A\,dS +$$

$$\int_{S_W} \delta A\,dS + M_\infty^2 \int_V \frac{G'}{R}\,dV \qquad (6\text{-a})$$

$$A = \Phi'\,\frac{\partial 1/R}{\partial n} - \frac{\dot{\Phi}'}{R}\,\frac{\partial T}{\partial n} \qquad (6\text{-b})$$

where the P.G. space coordinates must be considered, even if the symbols used for the physical coordinates are retained. As for the other symbols used in equations (6-a) and (6-b): the unit vector $\vec{n}$ is the outward normal to the aircraft surface S_B; $\psi = \partial\Phi/\partial n$; $\dot{\Phi} = \partial\Phi/\partial t$; R = distance between $P \equiv (x, y, z)$ and the centroid (x_1, y_1, x_1) of dS in the P.G. space;

$$T = [\,R + M_\infty\,(x - x_1)\,]\,M_\infty\,/\,[\,U_\infty(1-M_\infty^2)^{1/2}\,]\,; \qquad (6\text{-c})$$

the prime' indicates the value at the retarded time

$$t' = t - [\,R - M_\infty\,(x - x_1)\,]\,M_\infty/[\,U_\infty(1-M_\infty^2)^{1/2}\,]; \qquad (6\text{-d})$$

δA is the jump of A across the wake surface S_W ; V is the space outside $S_B + S_W$; E(P) = 1, ½, 0 if P lies outside, over or inside $S_B + S_W$, respectively.

As well known, the wake surface on which the trailing vortices associated with the lifting effects are positioned, must have a shape such that the balance equations are not violated.

As Morino claims, his equations(6), or his very similar equations for $M_\infty > 1$, can be used to compute a potential flow around a surface, which may be steady or unsteady (small displacements), in subsonic, transonic or supersonic flow. This possibility is one of the main reasons of our interest in Morino's method.

The basic feature of the linear methods is to reduce the dimension of the aerodynamic problem, i.e. the number of unknowns, of one order of magnitude, by locating the unknowns only on the surface of the configuration.

Let us consider equations(6) for the steady state conditions, neglecting the non linear terms (G=0). By replacing $S_B + S_W$ with a closed surface S we have, fig. 1 :

$$4\pi E(P)\,\Phi(P) = \int_S \left(-\frac{\partial\Phi}{\partial n}\frac{1}{R} + \Phi\,\frac{\partial 1/R}{\partial n}\right) dS \qquad (7)$$

Inside S we can define $\Phi = 0$ because we have E=0. Let H be a function defined inside and on S, continuous in the closed domain and such that $\nabla^2 H = 0$ inside S.

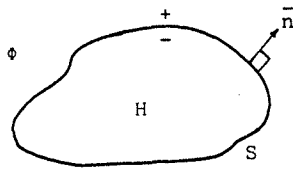

Fig. 1 : Scheme of the external and internal potential flow problems

We have:

$$4\pi\,[\,1 - E(P)\,]\,H(P) = \int_S \left(\frac{\partial H}{\partial n}\frac{1}{R} - H\,\frac{\partial 1/R}{\partial n}\right) dS \qquad (8)$$

Outside S we can define H = 0 because we have 1 - E = 0.

By putting:

$$\phi^{\pm} = E\,\phi + (1-E)\,H \qquad (9\text{-a})$$

$$q = \partial\phi/\partial n\,|^{+} - \partial H/\partial n|^{-}\ ,\quad m = H\,|^{-} - \phi|^{+} \qquad (9\text{-b,c})$$

where $|^{+}$, or $|^{-}$, indicate the limit values set on S from outside and inside respectively, from Eq.(7) and (8) we obtain :

$$4\pi\Phi^{\pm}(P) = -\int_S \frac{q}{R}\,dS - \int_S m\,\frac{\partial 1/R}{\partial n}\,dS \qquad (10)$$

Therefore, the vector field given by $\vec{v} = \nabla\Phi^{\pm}$, for points not belonging to the surface S, and by $\vec{v}\,|^{+}$ and $\vec{v}\,|^{-}$ on S, can be considered to be induced by sources of strength q and doublets (equivalent to elementary vortex rings) of strength m distributed on S. By changing H we do not change $\vec{v} = \nabla\Phi$ outside S, although we change the values of q and m.

Starting from Eq.(10) the subcritical panel methods may approach the solution of the aerodynamic problem by following two different schemes :

a) The classical one, which is called in this way because it was developed at an earlier time, but which is also termed "singularity method". In it the problem is reduced to the solution of a surface integral equation relating the unknown singularity strength to the normal wash on the surface of the aircraft, which is known from the boundary conditions.
The basic method of Hess & Smith[5] for non-lifting flows is of this kind. It is based on the formula for the source distribution:

$$4\pi\vec{v}(P) = -\nabla\int_{S_B} q\,\frac{dS}{R}\ , \qquad (11)$$

obtained from the equations (9) and (10) by choosing H such that $H|^{-} = \phi|^{+}$ on S. The NLR method[3], based on the works of Hess & Smith[5] and Rubbert & Saaris[6], is also of this kind and can be applied to lifting flows.

b) The "potential method", in which the potential on the surface is the unknown of the resolving integral equation directly derived by applying Green's theorem ; we get this integral equation by putting H = 0 in equations(9) and (10) with P on S (E(P)= ½) , and isolating the contribution of the wake :

$$4\pi E(P)\phi(P) = -\int_{S_B} \frac{\partial\Phi}{\partial n}\,|^{+}\,\frac{dS}{R} + \int_{S_B}\Phi|^{+}\,\frac{\partial 1/R}{\partial n}\,dS + \int_{S_W}\delta\Phi\,\frac{\partial 1/R}{\partial n}\,dS \qquad (12)$$

Eq.(12) is the reduced form of Eq.(6-a) when only linear terms are considered for steady flow.

We get $\partial\Phi/\partial n\,|^{+}$ from the boundary conditions. It must be noted that the integral equation is not obtained by imposing that the boundary conditions on the normal-wash be satisfied, but rather by making use of the continuity of the potential Φ when P approaches S.

The panel program S-SUB2 developed at the University of Pisa and based on Morino's method, is of this type.

The treatment of flows around lifting bodies, hence with non-zero circulation, requires that a discontinuity in the velocity potential φ be present in the flow field. This discontinuity occurs on the wake which is represented by horse-shoe vortices trailing from the edges of all lift-carrying parts of the configuration. The value of the circulation, hence the intensity of the wake vortices, is determined by imposing the Kutta condition, which may take different forms.

In the panel methods the surfaces S_B and S_W are approximated by polyhedral surfaces the faces of which are termed "panels". On each panel, the singularity may have constant, linear, or quadratic changing strength.

2.2. Theoretical main features of the two panel methods

Both in Morino's and the NLR methods considered, the shape of the wake is fixed in order to maintain the problem linear: it is possible to demonstrate that the so introduced errors are negligible in most practical cases.
It would however be possible to determine the correct wake shape by an iterative process, if necessary.

In Morino's method[1,4] there is no paneling difference between lifting and non lifting surfaces or bodies, except for the wake, which is added to the lifting components. In the NLR formulation[3] the horse-shoe vortex system representing the wake is prolonged into the lifting surfaces and intersecting bodies; then a skeleton surface is defined for all wing-like components.
Consideration is first given to Morino's Eq.(12). The doublet intensity $\delta\Phi$ is constant on each semi-infinite strip (equivalent to a horse-shoe vortex) of the wake S_W The boundary conditions are applied to a finite number of points located at the centroids of the quadrilateral panels, fig. 2, generally having the shape of hyperbolic paraboloids. The values of $\phi|^{+}$ and $\partial\phi/\partial n|^{+}$ are assumed to be constant on each panel. The value of the normal-wash $\partial\Phi/\partial n\,|^{+}$ is given by the boundary condition; the value of $\phi|^{+}$ can be found by solving a system of N linear equations in N unknowns, where N is the number

of panels on S_B.

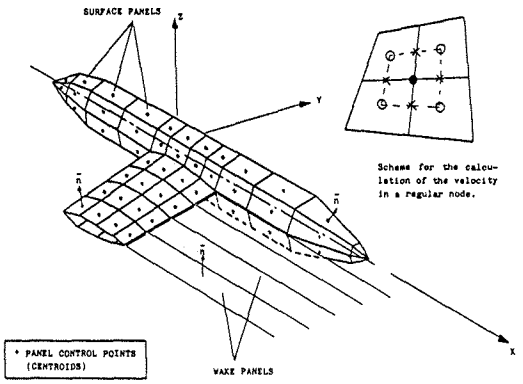

Fig. 2 Scheme for Morino's method

In Morino's formulation there is no need for an explicit Kutta's condition: the only requirement being that the potential Φ has the same values on the wake faces and on the adjacent body panels. This condition yields $\delta\Phi$ on the wake, which is prolonged in the direction, for instance of the trailing edge bisector, or of the asymptotic flow, and is not prolonged into the configuration.

Under these conditions vortices passing through a panel in areas very close to the control points are no longer present. Imagining a wake surface trailing from a fuselage or a pod, which can thus be thought as a "lifting part", is fully acceptable.

The velocity can be found by differentiation of Φ and the pressure from Bernoulli's equation. In the program developed at the University of Pisa for steady flows, the velocity is computed at the nodes and not at the centroids of the panels. For each regular node (belonging to four panels), the velocity is given by two crossed differences of the velocity potential on S_B, as shown in fig. 2.

This procedure may be adapted for non-regular nodes, but in such a case it is liable to yield a poor accuracy.

Morino's method allows an alternative calculation of the section-lift coefficient, based on the Kutta-Joukowski formula to be made:

$$C_l = 2\frac{\Gamma}{U_\infty c} = 2\frac{\Phi_N - \Phi_l}{U_\infty c} \qquad (12)$$

where Φ_N and Φ_l are the (perturbation) velocity potentials at the upper and lower panels near the trailing edge. The so obtained results are usually more accurate than the ones calculated by integration of the pressure coefficients without a fine paneling.

Consideration is now given to the NLR method[3,7]. A surface source distribution, which takes into account the thickness effects of the wings and the volume effects of the bodies, is coupled with a vortex lattice which takes into account for the lift effect (fig. 3).

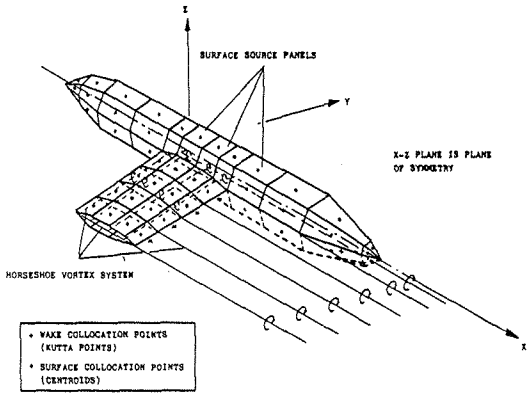

Fig. 3 Scheme for the NLR method

Each quadrilateral panel of the discretized model for the surface S_B carries only a constant source distribution, the influence of which is directly computed in terms of velocity. The source strength is variable from one panel to the following. As said before, the system of horse-shoe vortices is prolonged into the lifting surfaces and the intersecting bodies, distributing the vortices on the skeleton surface which is defined for all wing-like components.

A parabolic weight function of the bounded vorticity distribution per segment is assumed, which vanishes near the trailing edge. The internal vortex sheet is prolonged reaching a position not nearer to the leading edge than 0.5% of the local chord. The entire vortex distribution is determined by one unknown quantity per segment, i.e. the total circulation around the segment. The unknown strength of the sources and circulations is determined by imposing the flow-tangency condition at the centroids of the panels of S_B and the Kutta condition. This condition is imposed by requiring that the velocity be tangent to the wake surface close to the trailing edge of the lifting surfaces; the wake vortex sheet is prolonged along the trailing edge bisector and, on each wake strip, the control point is located at a distance of about 0.3% of the local chord. The bound vortices lie along the spanwise panel edges and the trailing vortices lie along the streamwise segment edges, but the vortex at the tip is placed inboard of the tip at 10% of the spanwise panel width.

Generally, vortex systems of intersecting lifting surfaces have to be connected. As well known, in the case of lifting bodies it may be difficult to define a starting position of the vortex sheet. Therefore, when the NLR method is implemented to wing-body combinations it is assumed that a vortex sheet is located behind

the body, which is a continuous prolongation of the sheet of the wing.

To avoid singular behaviours, the trailing-edge of the lifting surfaces is opened. Crude paneling near the trailing edge must be avoided as a possible strong interference may arise between adjacent sources and vortices. The NLR method usually does not yield good results when applied to thin airfoils. If the wing is relatively thin it is necessary that it is represented by a fairly large number of chordwise panels in order to produce a reliable pressure distribution.

Finally, as far as the compressibility corrections are concerned, in the computational process of both the NLR and Morino's methods the configuration is first transformed into the P.G. space. The incompressible potential flow solution in this space must be corrected to obtain the final aerodynamic quantities in compressible flow, such as pressure distribution, lift and pitching moments. In Morino's formulation the correction is made by Göthert's rule. In the NLR method a better correction is made by a semi-empirical modified Göthert's rule which permits satisfactory results up to the critical Mach number to be obtained. The greatest differences in pressure distributions given by the two compressibility rules may be expected to be found near the wing leading edge. In this area the condition requiring that the local disturbances must be small with respect to the local speed of sound, may be easily violated and the compressible suction obtained with the simple Göthert's rule may be overestimated.

2.3. Numerical main features of the two panel methods

In practice both methods require the solution of an rather large system; matrix size can be typically approximately 1000 x 1000 for a complex configuration.

NLR program uses an iterative Gauss-Seidel solution algorithm, while the program S-SUB2 developed at the University of Pisa and based on Morino's formulation relies on a direct solution.

This difference is not very significative from the theoretical point of view since it mainly affects the memory core requirement; an iterative solution could however be highly desirable on smaller machines such as Aermacchi's UNIVAC 1100/80, if virtual memory addressing is to be avoided.

The rate of convergence with respect to the number of panels for both methods can be considered the same (the error should decrease roughly in proportion to 1/N where N is the number of panels).

Morino's method is thought to require in general a smaller number of panels to model a configuration.

Another feature from the practical point of view in Morino's method is that velocity has to be derived by differentiation or by difference. The value of Φ at 4 adjacent panel centroids may be used to calculate the velocity in correspondence to the common vertex (regular point); special care is to be taken in computing velocity values at edges and non-regular points.

Moreover, the NLR program is an effective, industrial tool, with an optimized iterative schemes, while the program developed at the University of Pisa is still a research program and as such, requires a lot of facilities, the most important of which is an iterative solution of the system.

3. Wind Tunnel Testing

The geometry chosen for the check of the performance of the two numerical programs is a wind tunnel model built for the accomplishment of a series of tests in the A.R.A. 9 ft x 8 ft (2.74 m x 2.44 m) transonic tunnel in the development phase of a new close-air support aircraft.

The model in 1:7 scale, named M3, was designed to supply a complete set of data on aerodynamics, stresses, performance and flight mechanics, at a Re $\simeq 3.5 \cdot 10^6$, and up to a Mach of 0.925.Model M3 depicted in fig. 4, offered the following advantageous pecularities:

- good aerodynamic reliability ensured by the possibility of testing at fairly large scale, which allows high Reynolds numbers and a more accurate reproduction of excrescences and configuration details;
- easy of accomodation of all balances and pressure tubes within the confines of the model surfaces, as well as the possibility of achieving a larger mass flow in the internal duct.

The model dimensions were governed by the model size to tunnel ratio, model blockage to tunnel area ratio, and loading limits of balance and sting support.

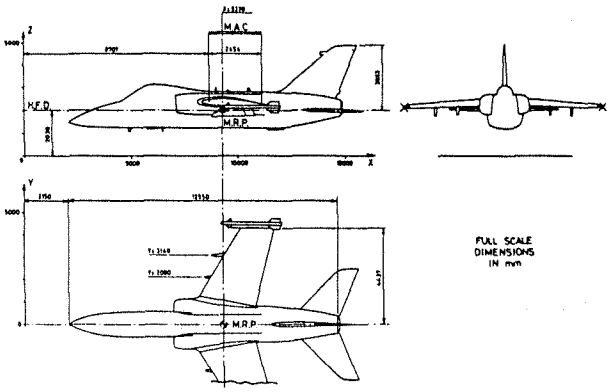

Fig. 4 Aircraft three views

In fact model M3 was designed to attain the following :

a) overall load measurements;

b) definition of the aerodynamic loads on control surfaces, pylons, missiles and external stores;

c) surface pressure measurements;

d) variable flow through the internal duct.

In particular a total number of 400 surface pressure points were fitted to the model starboard side, of which approximately 150 were fitted to the fuselage and 250 to the wing. The fuselage pressure measurement stations are shown in fig. 5.

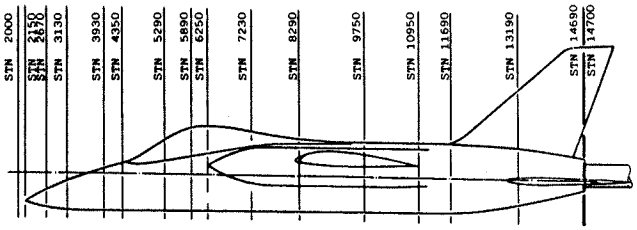

Fig. 5 Fuselage pressure measurement stations

The six wing pressure measurement stations are shown in fig. 6, which also shows the relative positions of the wing control surfaces in the cruise configuration.

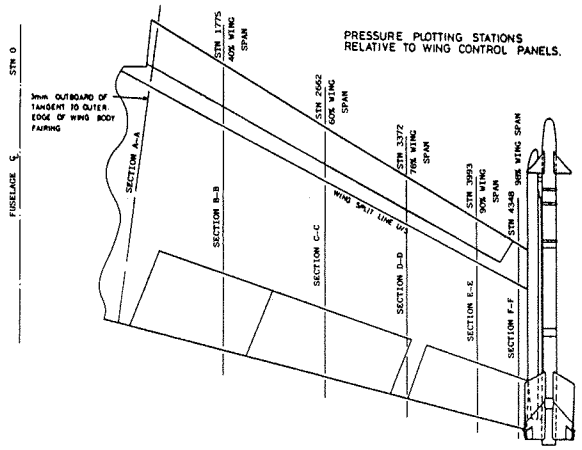

Fig. 6 Wing pressure measurement stations

A picture of the positions of the upper and lower surface pressure points for each station is shown in fig. 7.

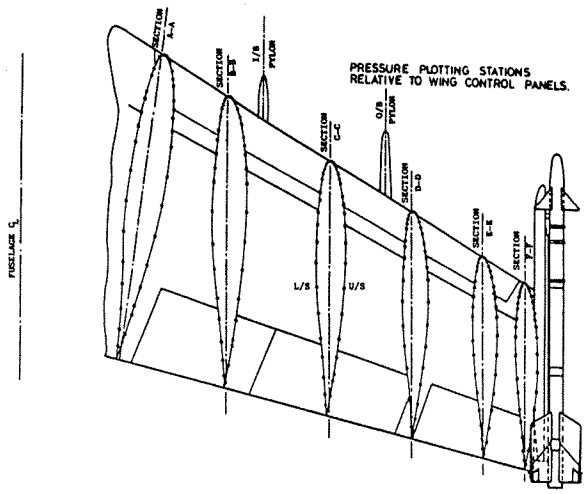

Fig. 7 Layout of wing pressure measurement points

The pressure measurements, integrated in chord and span on the wing or across and along the fuselage, allow a comparison with the loads measured by the internal balances on the single surfaces and a check of the carryovers evaluated by theoretical methods.

For these reasons model M3 appears suitable to study complex 3-D subcritical or supercritical flow fields (wing-body, wing-pylon, wing-missile junctions) and the effects of the external stores on both the local flow fields and the overall aerodynamic characteristics.

4. Panel schemes and computing time

The discretized geometry schemes utilized in this comparison are very similar for the two computer programs, with the obvious differences dictated by their different structure. This means that special care was taken to ensure the same level of detail in describing a given part of the configuration, although the location of panel corners and control points may differ.

Two of these schemes were prepared to examine pressure and load distributions on the fuselage with a simplified representation of the wing. The first one, depicted in fig. 8, includes about 550 panels on the fuselage; the second (fig. 9) has about 300 panels. The number of panels for the wing was chosen in order to correctly represent the interference effects on the fuselage.

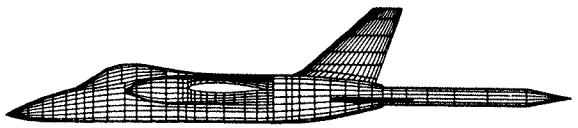

Fig. 8 Fine fuselage scheme for the NLR program (Clean wing) - Scheme 1

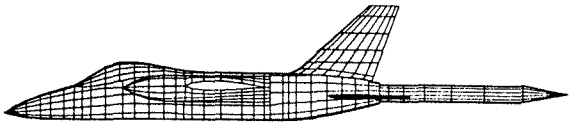

Fig. 9 Simplified fuselage scheme for the NLR program (Clean wing) - Scheme 2

Note that both schemes directly represent the wind tunnel model rather than the real aircraft, and are therefore fitted with air intake fairing and caudal sting support.

Since only symmetrical cases were considered (no sideslip)the vertical tail is not represented as a lifting surface but as part of the body.

Fig. 10 shows the first scheme devised for wing analysis. 270 (9x30) panels are on the wing in the case of Morino's method, and 240 (8x30) panels in the case of the NLR method. A front view is shown in Fig. 11. The different spanwise paneling was realized in order to meet the same spanwise experimental stations, taking into account the different points at which the pressure coefficients are calculated (corner points for the S-SUB2 program, panel centroids for the NLR program).

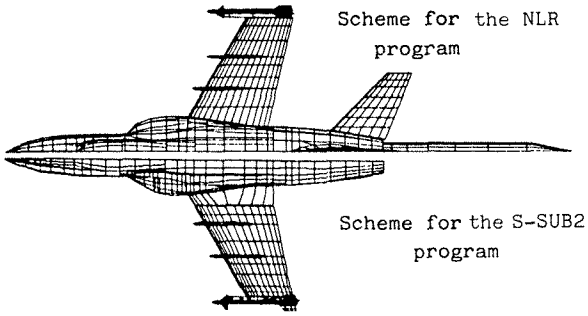

Fig. 10 Complete configuration scheme 15+15 chordwise wing panels

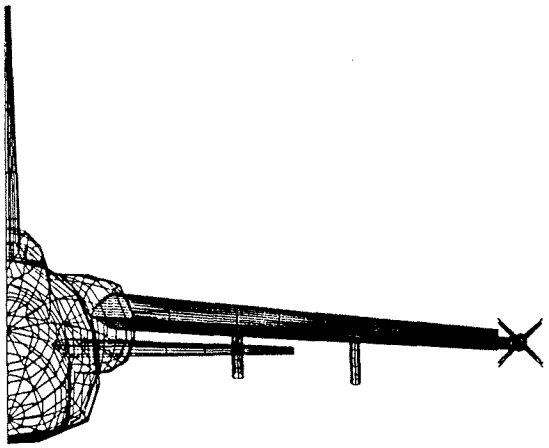

Fig. 11 Complete configuration scheme for the NLR program - Frontal view

The pylons are represented as lifting surfaces to take accurately into account spanwise flow effects; each of them carries its roper vortex system; rear missile fins are also lifting, while the front ones are not so. This option had to be adopted to avoid trailing vortex interference problems which could severely affect the solution accuracy near the wing tips, and because it was felt that full missile fin lift modeling would in any case have merely a strong but very localized effect on the pressure distribution over the missile body and at the wing tip.

The second scheme used for wing analysis was obtained by reducing the number of chordwise panels from 15+15 to 10+10 (Fig. 12). This was thought to be the minimum number capable of permitting the profile geometry to be correctly represented.

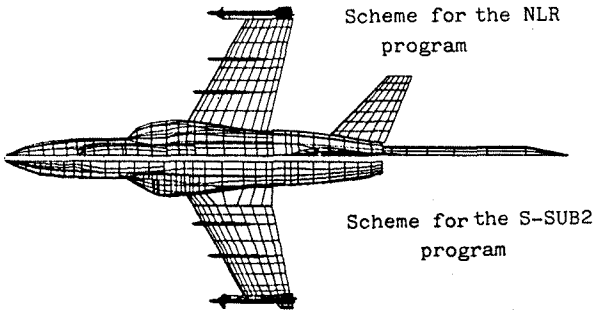

Fig. 12 Complete configuration scheme 10+10 chordwise wing panels

To simplify data reduction and to minimize interpolation problems, the panel strips have been located at the pressure measurements stations of the model whenever this was possible without unnecessary complications. This explains the somewhat "uneven" appearence of the panel distribution in all the schemes.

Finally, it may be worth remarking that the schemes were produced directly from a digitized geometry data base using Aermacchi's CAD/CAM system. This, of course, dramatically cuts the time and costs involved in modeling and modifying the geometry.

Computing times are given in Fig. 13, for the different panel schemes used for the pressure calculations with the two methods.

The data refer to a case of one Mach number and two incidences (α).

The runs were performed on two different computers, the NLR on UNIVAC 1100/80 and the other on IBM 370/168:the times are not directly comparable, even if a sample test case (about 300 panels) in which Morino's method was used, was run on both computers, and the total time on UNIVAC was found to be three times higher.

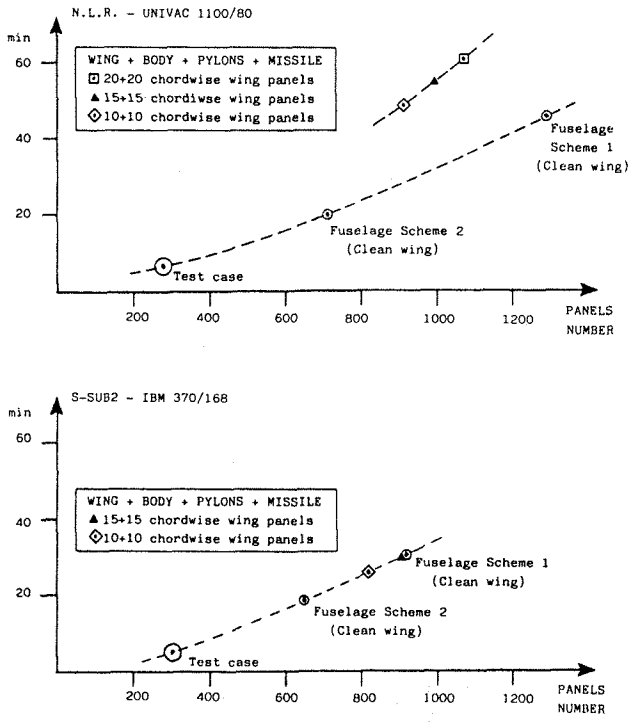

Fig. 13 Computing times for the NLR and S-SUB2 programs

The two methods were applied to the same test case which was then run on the UNIVAC 1100/80: the total computing time taken by the program developed at the University of Pisa was found to be about four times higher than that taken by the NLR program.

This remarkable difference is probably due to the fact that the program developed at Pisa is still a general purpose and research program including a lot of controls and options for future development, and that the system of equations is solved directly. For this program, in fact, more than 2/3 of the total computing time was used to prepare the influence matrix, while this operation is performed in the NLR program in less than 1/3 of the total time required.

A marked increase in the computing time taken by the NLR method was found when interfering lifting surfaces, such as wing plus pylons were treated: this was due to an increase in the numbers of iterations needed to reach convergence (see fig. 13).

No significant difference in computing time was found between the analogous configurations calculated with Morino's method.

The core memory required to run the NLR program is of 50-70 Kwords, rather insensitive to the number N of panels (the increase is about 10*N words), while that needed by the S-SUB2 program is about $(900 + \frac{3.5}{1000} \cdot N^2)$ Kwords for the IBM 370/168 computer.

5. Comparison of results

Pressure distributions on wing and fuselage computed by using both the NLR and the S-SUB2 programs, were compared with wind tunnel data at the same experimental wing-spanwise or longitudinal sections.

The comparison of the pressure distribution was made at Mach = 0.7, α = 0°, 5° for the fuselage and Mach = 0.5, α = 0°, 5° for the wing, to avoid supercritical pressure coefficients on the wing at higher α.

Typical wind tunnel pressure distributions measured on the upper surface of the wing with two incidences, α = 0° and 5°, Mach = 0.5, are shown in figure 14, where measurement stations B, C, D, E, F are indicated.

The effect of the vortex system induced by the missile near the wing tip (see station F) can be identified even if the missile shape is not represented.

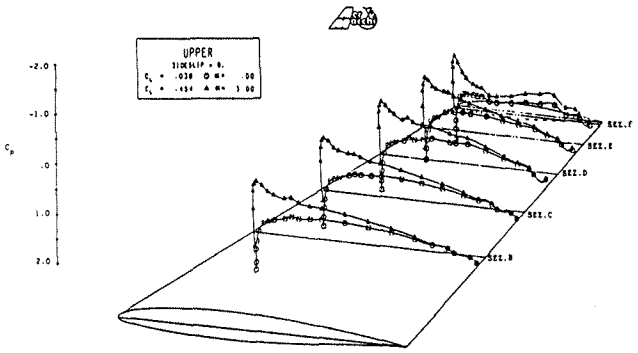

Fig. 14 PRESSURE DISTRIBUTIONS ON WING, MOD. M3, MACH = 0.5
HIGH SPEED WIND TUNNEL TEST RESULTS (A.R.A. T.N. 74151)

In the following figures there are compared the chordwise pressure distributions at station C only, as this station can be considered a representative wing section. C_{NLOC} and C_{MLOC} represent the local normal force and the pitching moment coefficient. C_{MLOC} is assumed positive upward and referred to 25% of the local chord from the leading edge. Calculated pressure distributions at station F failed in reproducing the complex flow field locally induced by the tip missile, as it could be expected.

In figures 15 and 16 the experimental pressure distributions are compared with the computed ones obtained through the NLR program. The computed results shown in fig. 16 were obtained at an incidence lower than the experimental one. This case was run to match with good approximation the local normal force coefficient (C_{NLOC}), and it is possible to note that the agreement with the experimental results is much more satisfactory, as far as both low and high incidence are concerned.

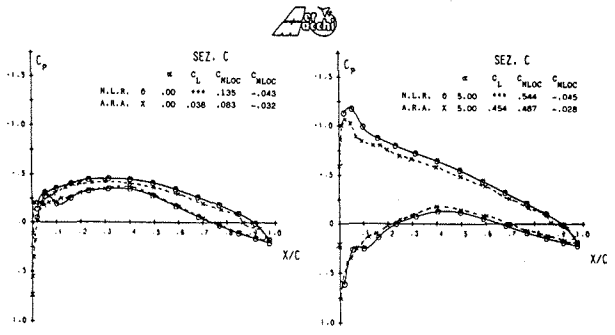

PRESSURE DISTRIBUTIONS - CRUISE WING
Fig. 15 THEORETICAL RESULTS FROM N.L.R. PANEL PROGRAM (15+15 CHORDWISE PANELS) MACH = .500
HIGH SPEED WIND TUNNEL TEST RESULTS (A.R.A. T.N. 74151)

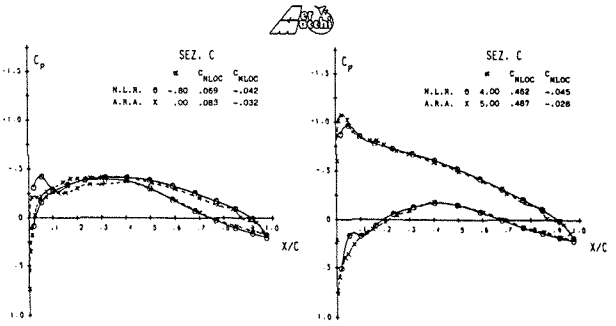

PRESSURE DISTRIBUTIONS - CRUISE WING
Fig. 16 THEORETICAL RESULTS FROM N.L.R. PANEL PROGRAM (15+15 CHORDWISE PANELS) MACH = .500
HIGH SPEED WIND TUNNEL TEST RESULTS (A.R.A. T.N. 74151)

As shown in Fig. 17 the incidence correction affords a better agreement for the other spanwise stations as well. A similar result was yielded for the computed pressure distributions obtained by use of the S-SUB2 program. The agreement between the computed and the experimental lift curve slopes is however satisfactory.

Presently this "shift of incidence" effect is still being investigated.

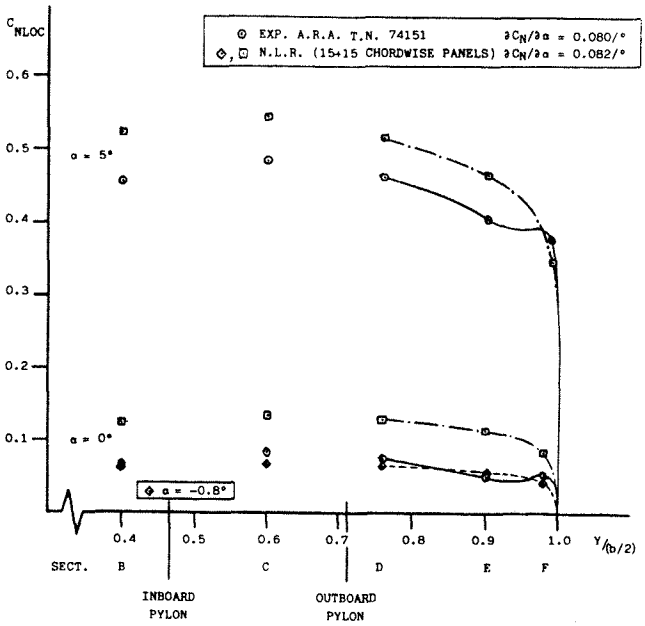

Fig. 17 Spanwise load distribution

The fig. 18 shows the comparison between the experimental pressure distributions and the distributions computed using the S-SUB2 program. In fig. 19 conversely there are compared the same results of the S-SUB2 program and those obtained with NLR program. As can be seen from figures 18 and 19 the S-SUB2 program overesti mates the suction at the leading edge, probably because the simple Göthert's rule is inadeguate to correct for the compressibility effects near the leading edge.

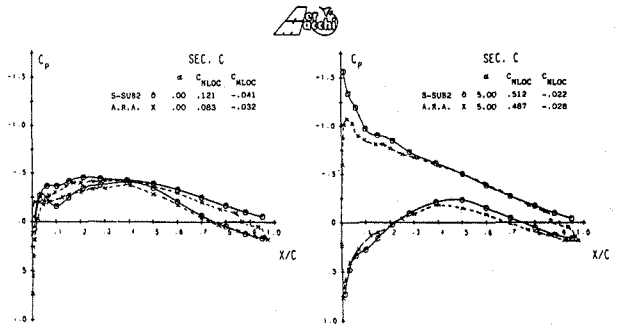

PRESSURE DISTRIBUTIONS - CRUISE WING
Fig. 18 THEORETICAL RESULTS FROM S-SUB2 PANEL PROGRAM (15+15 CHORDWISE PANELS) MACH = .500
HIGH SPEED WIND TUNNEL TEST RESULTS (A.R.A. T.N. 74151)

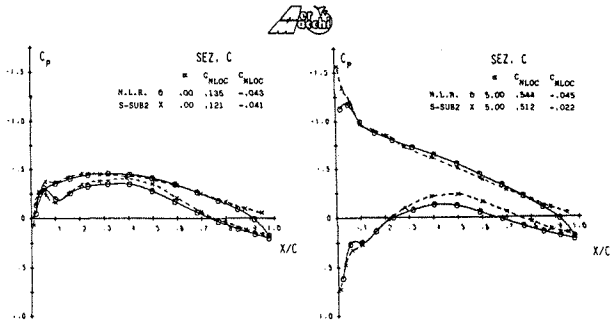

PRESSURE DISTRIBUTIONS - CRUISE WING
Fig. 19 THEORETICAL RESULTS FROM N.L.R. PANEL PROGRAM (15+15 CHORDWISE PANELS) MACH = .500
THEORETICAL RESULTS FROM S-SUB2 PANEL PROGRAM (15+15 CHORDWISE PANELS)

In figures 20 and 21 the different chordwise paneling effect is shown for the NLR and the S-SUB2 programs. This effect is negligible for the S-SUB2 program, while some difference is found for the NLR program.

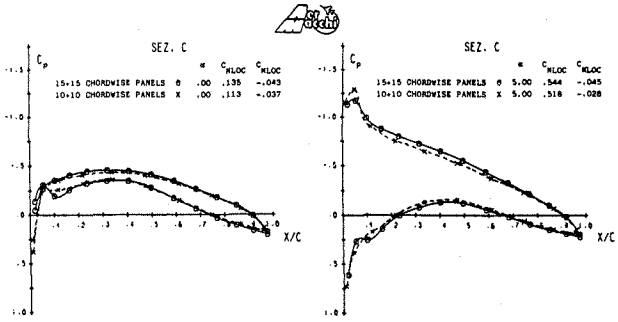

PRESSURE DISTRIBUTIONS - CRUISE WING
Fig. 20 THEORETICAL RESULTS FROM N.L.R. PANEL PROGRAM MACH = .500

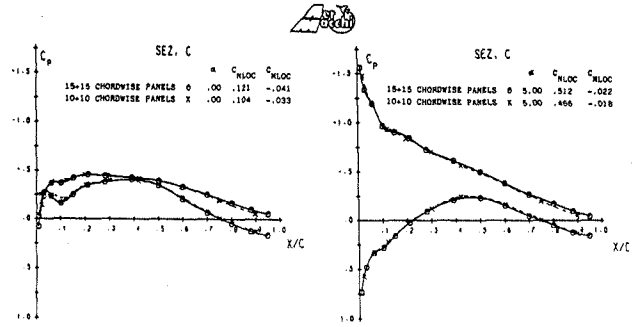

Fig. 21 PRESSURE DISTRIBUTIONS - CRUISE WING
THEORETICAL RESULTS FROM S-SUB2 PANEL PROGRAM MACH = .500

In figures 22 and 23 the calculated and experimental pressure distributions for a typical fuselage section are compared. Figure 22 shows the experimentally measured values and the shape of the fuselage cross section. Figure 23 compares the results obtained with the NLR and S-SUB2 programs, using a fine (scheme 1, fig. 8) and a coarse (scheme 2, fig. 9) fuselage paneling. The paneling effect is negligible, while there are small differences between computed and experimental results.

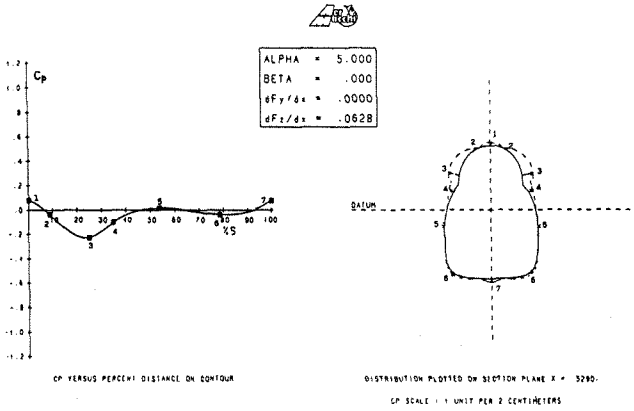

PRESSURE DISTRIBUTIONS ON FUSELAGE SECTIONS - MOD. M3
HIGH SPEED WIND TUNNEL TEST RESULTS (A.R.A.) - CRUISE MACH = .70

Fig. 22

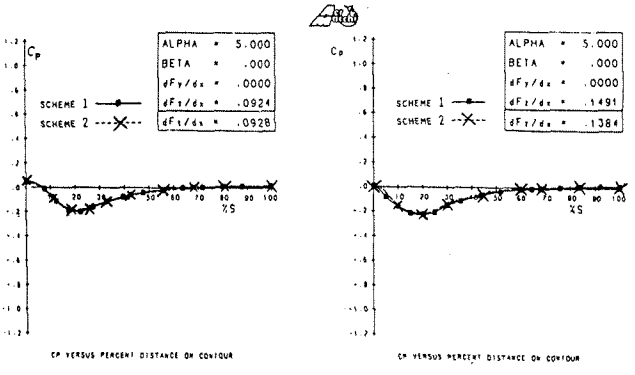

PRESSURE DISTRIBUTIONS ON FUSELAGE SECTION X = 5290 MACH = .700
THEORETICAL RESULTS FROM N.L.R. PANEL PROGRAM THEORETICAL RESULTS FROM S-SUB2 PANEL PROGRAM

Fig. 23

In figures 24 and 25 the calculated and experimental pressure distributions for another typical fuselage section, at wing-body junction, are compared.
The agreement is good, even if the S-SUB2 program shows some difficulties in defining the C_p values near wing-body junction, due to the necessity of calculating the speed at irregular nodes.

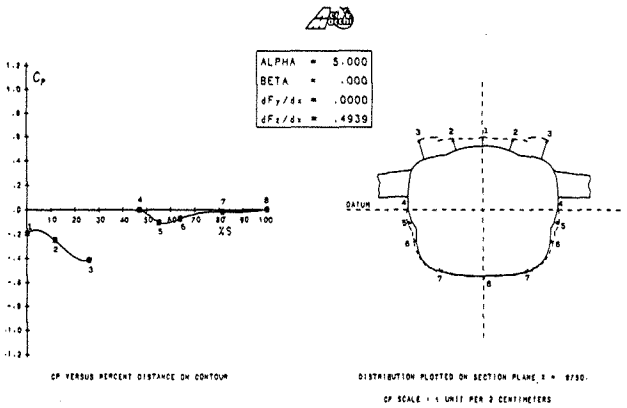

PRESSURE DISTRIBUTIONS ON FUSELAGE SECTIONS - MOD. M3
HIGH SPEED WIND TUNNEL TEST RESULTS (A.R.A.) - CRUISE MACH = .700

Fig. 24

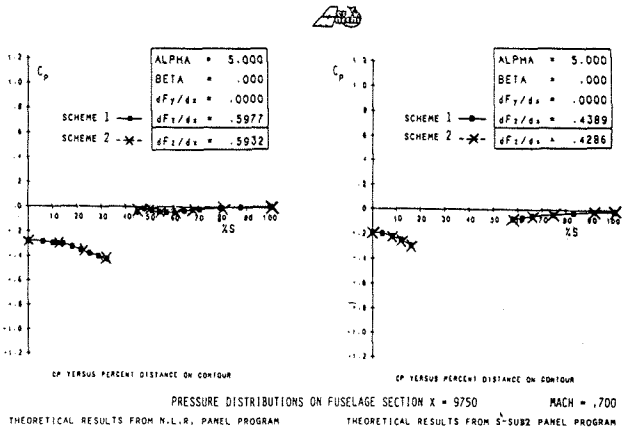

PRESSURE DISTRIBUTIONS ON FUSELAGE SECTION X = 9750 MACH = .700
THEORETICAL RESULTS FROM N.L.R. PANEL PROGRAM THEORETICAL RESULTS FROM S-SUB2 PANEL PROGRAM

Fig. 25

Figure 26 gives an example of the longitudinal normal force distribution along the fuselage, obtained by integrating the experimental and the computed pressure distributions over the fuselage cross sections. The numerical results appear less satisfactory near the body-wing leading edge junction, where the complexity of the aircraft shape would require a higher number of panels.

An example of the influence of fuselage paneling is shown in fig. 27, where the results obtained with the two schemes used for fuselage pressure calculations are compared.

The sensitivity to fuselage paneling appears negligible, except at particular sections.

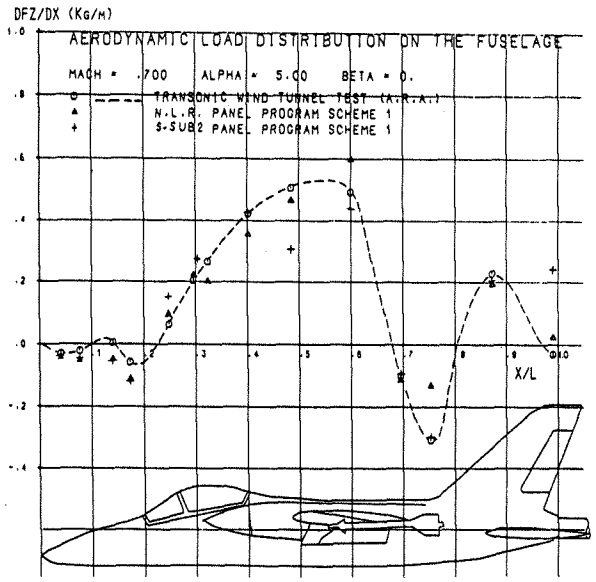

Fig. 26

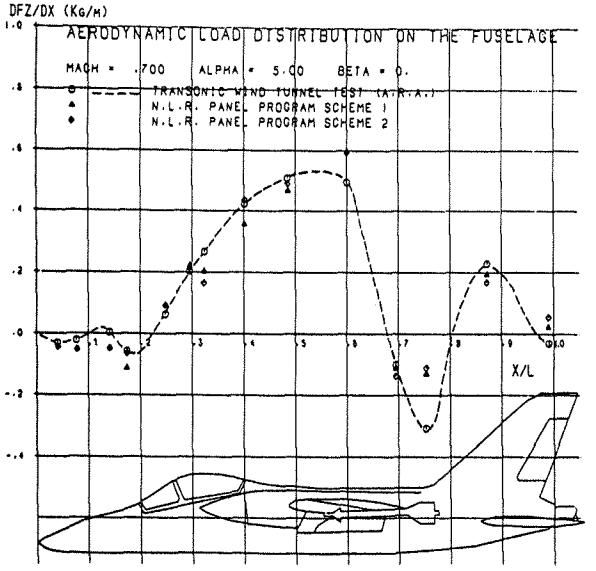

Fig. 27

6. Conclusions

A comparison between the results obtained with two first order panel programs and wind tunnel data for a complex fighter aircraft configuration has been reported. This configuration was mainly chosen because a large amount of detailed experimental data was available. The two computer programs used are a panel program, herein named NLR, based on the "singularity method", and another program, named S-SUB2, based on the "potential method".

The optimization of the panels distribution was conditioned by the maximum number of panels (about 1000) imposed by the present characteristics of the S-SUB2 program (core memory and computing time limits) and by the requirement to meet the experimental measurement stations (in order to avoid further interpolations). These limits have prevented the accomplishment of a more complete analysis of the influence of panels density on the numerical results. However, in the regions where the flow is not too complex, the computation results have confirmed that the S-SUB2 program, based on the "potential method", has a lower sensitivity to the panel density and distribution. In these regions the results of both the computer programs are in good agreement with the experimental results, the differences being likely to be ascribable to the boundary layer effects.

As far as the compressibility effects are concerned, the S-SUB2 program requires a more accurate correction than Göthert's rule.

Finally the NLR program has shown to be an effective industrial tool, while the S-SUB2, which is yet a research program, still needs a lot of facilities, the most important of which is an iterative solution of the algebraic system to reduce core and time requirement.

Acknowledgments

The authors wish to thank Mr. O. Comte de Resende, visiting Engineer at Aermacchi from Embraer, and Mr. E. Artoni, Aermacchi Engineer, for their collaboration, and Mrs. M.R. Mazzoni and Mrs. R. Fischer for manuscript preparation.

References

[1] Morino, L., Kuo, C.C. "Subsonic Potential Aerodynamics for Complex Configurations : a General Theory". AIAA Journal, Feb. 1974.

[2] Bindolino, G., Mantegazza, P., Visintini, L. "A Comparison of Panel Methods for Potential Flow Calculations". AIDAA Conference Proceedings, Turin (Italy), September 23-27, 1985.

[3] Labrujere, Th. E., Loeve, W., Sloof, J.W. "An Approximate Method for the Calculation of the Pressure Distribution on Wing-Body Combinations at Subcritical Speeds". AGARD CP 71-71, September 1970.

[4] Lombardi, G., Polito, L. "Calculation of Steady and Unsteady Aerodynamic Loads for Wing -Body Configurations at Subcritical Speeds". AIDAA Conference Proceedings, Naples (Italy) 1983, Vol. 1, pp. 209-222.

[5] Hess, J.L., Smith, A.M.O. "Calculation of Potential Flow about Arbitrary Three-Dimensional Bodies" Douglas Aircraft Corp. Rept. ES 40622, 1962.

[6] Rubbert, P.E., Saaris, G.R. "A General Three -Dimensional Potential Flow Method applied to V/STOL Aerodynamics" S.A.E. Paper 680304,1968.

[7] NLR Memorandum AT-83-003U "Program Panel Version 1.0. User's Guide", 1983

[8] Tseng, K., Morino, L. "Non Linear Green's Function Method for Unsteady Transonic Flows" Transonic Perspective Symposium, California, Feb. 18-20, 1981.